Journal of Mechanical Design | Volume 130 | Issue 9 | Research Paper

Unified Uncertainty Analysis by the First Order Reliability Method

Xiaoping Du

Department of Mechanical and Aerospace Engineering
University of Missouri – Rolla
1870 Miner Circle
Rolla, Missouri 65409 – 4494
Phone: (573) 341-7249
Fax: (573) 341 - 4607
E-mail: dux@umr.edu

Original version: May 2006
1st revision: September 2006
2nd revision: February 2007

Abstract

Two types of uncertainty exist in engineering. Aleatory uncertainty comes from inherent variations while epistemic uncertainty derives from ignorance or incomplete information. The former is usually modeled by probability theory and has been widely researched. The latter can be modeled by probability theory or non-probability theories and is much more difficult to deal with. In this work, the effects of both types of uncertainty are quantified with belief and plausibility measures (lower and upper probabilities) in the context of evidence theory. Input parameters with aleatory uncertainty are modeled with probability distributions by probability theory. Input parameters with epistemic uncertainty are modeled with basic probability assignments by evidence theory. A computational method is developed to compute belief and plausibility measures for black-box performance functions. The proposed method involves the nested probabilistic analysis and interval analysis. To handle black-box functions, we employ the First Order Reliability Method (FORM) for probabilistic analysis and nonlinear optimization for interval analysis. Two example problems are presented to demonstrate the proposed method.

1. Introduction

Products must be reliable, robust, and safe against uncertainties. To this end, nondeterministic design approaches have been increasingly researched and applied by industry, government, and academia [1-3]. Uncertainty can be viewed as the difference between the present state of knowledge and the complete knowledge [4]. Uncertainty is usually classified into aleatory and epistemic types [4-6]. *Aleatory uncertainty*, also termed as objective or stochastic uncertainty, describes the inherent variation associated with a physical system or environment. *Epistemic uncertainty*, or subjective uncertainty, on the other hand, derives from some level of ignorance or incomplete information about a physical system or environment.

Uncertainty associated with a parameter can be aleatory (due to the inherent variation) or epistemic (due to limited information). Uncertainty associated with a model structure is a special type of epistemic uncertainty [7-9], which comes from assumptions or a lack of knowledge in the model building process. Aleatory uncertainty is usually modeled by probability theory while epistemic uncertainty can be modeled by probability or non-probability theories.

Quantifying and managing the effect of uncertainty at the design stage is important – sometimes imperative – as in reliability-based design. Probabilistic approaches that deal with stochastic (aleatory) parameter uncertainty have been vastly investigated. Representative but not exhaustive methods include robust design [10-14], reliability-based design [15-17], and multidisciplinary optimization under uncertainty [18-20].

However, aleatory parameter uncertainty is only one facet of the total uncertainty that engineers encounter. The integration of a full range of uncertainty has barely been explored in engineering design. It is difficult to quantify epistemic uncertainty because the information may come from multiple sources and may be conflicting. Although a few theories of epistemic uncertainty are available, their practical engineering applications have scarcely been exploited. In addition, incorporating uncertainty into simulation-based design may lead to severe numerical difficulties because of the black-box nature and a high computational cost.

Exploratory research on epistemic uncertainty in engineering has recently been conducted. Several examples include (1) studies on the relationships and differences between probability and non-probability theories [21, 22]; (2) study on bounding the value of information with epistemic distribution parameters [23]; (3) optimization design by possibility and evidence theory [24, 25]; (4) sensitivity analysis with aleatory and epistemic uncertainties [26]; and (5) epistemic uncertainty in engineering applications [27, 28]. The above work has indicated the promising possible engineering applications of the treatment of a full range of uncertainty.

Evidence theory is a more general theory that can handle both types of uncertainty. However, it requires much more computational demands than the less general theory, namely, probability theory [29]. Monte Carlo simulation is capable of handling both types of uncertainty, but generally prohibitively expensive for real-world problems. Interval arithmetic combined with probabilistic analysis is efficient but may not be accurate and inapplicable to black-box models.

We propose a unified uncertainty analysis method based on the First Order Reliability Method (FORM). The method is referred to as FORM-UUA (FORM-Based Unified Uncertainty Analysis) in the rest of the paper. In FORM-UUA, aleatory uncertainty is modeled by random variables with distributions, and epistemic uncertainty is modeled by intervals with basic probability assignments. With coupled probabilistic analysis and interval analysis, FORM-UUA is able to quantify the effects of both types of uncertainty. To deal with a black-box performance function with high robustness, probabilistic analysis is performed by the improved HL-RF (iHLRF) algorithm [30]; interval analysis is embedded in the iHLRF algorithm and is conducted by nonlinear optimization.

A brief overview of evidence theory from a perspective of uncertainty analysis is given in Section 2. The unified uncertainty analysis framework, where the proposed method is derived, is presented in Section 3. The FORM-UUA method is discussed in Section 4 followed by two engineering examples in Section 5. Conclusions and possible future research are presented in Section 6.

2. Intervals and Evidence Theory

Intervals are widely used for epistemic uncertainty. Typical interval examples are given in [31]. The periodic condition monitoring is used herein to demonstrate the basics of intervals and evidence theory. The condition of a system is monitored at preplanned time instants t_0, $t_{1,}$ t_2, $\cdots$ as shown in Fig. 1. If a failure is detected at t_{i+1}, we know that the failure could occur at any instant over the interval between t_i and t_{i+1}. Epistemic uncertainty therefore exists in the estimation of the time to failure.

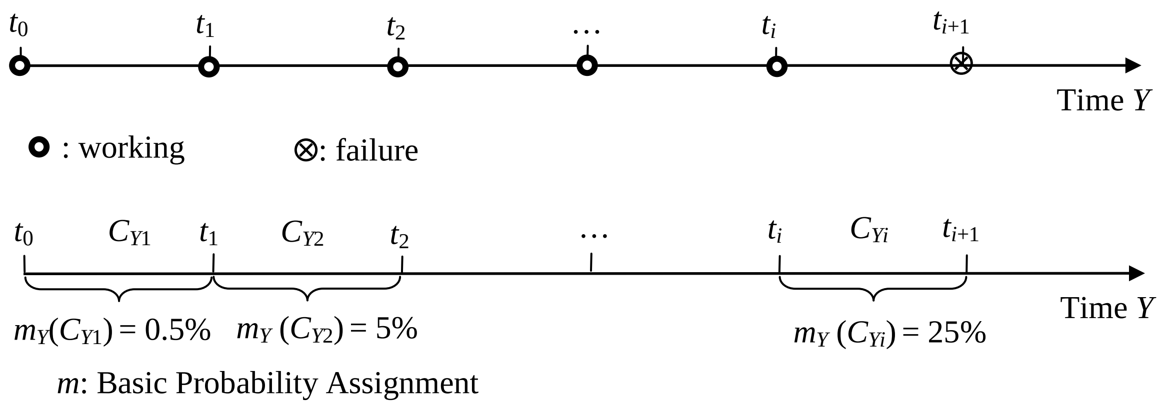

Figure 1. Periodic condition monitoring

We use Y to denote an epistemic parameter as well as its sample space, a space that contains all possible values of Y. The power set of Y, denoted by $\mathcal{P}(Y)$, contains all the possible distinct subsets of Y. For the above example, possible subsets of Y include $\{\varnothing\},\{C_{Y1}\},\cdots,\{C_{Yi}\},\{C_{Y1},C_{Y2}\},\{C_{Y2},C_{Y3}\}\cdots,\{C_{Y1},C_{Y2},\cdots,C_{Yn}\}$, where $\{\varnothing\}$ is an empty set, and n is the total number of subset $\{C_{Yi}\}$.

A probability (or belief), $m_Y(C_{Yi})$, can be assigned to each of the subsets $\{C_{Yi}\}$ $(i=1,2,\cdots,n)$ based on statistical data or engineering judgment. $m_Y(C_{Yi})$ is called a *Basic Probability Assignment* (BPA). The formal definition of BPA is as follows. A BPA, $m_Y(A)$, of a set A over a frame Y, is a mapping function: $\mathcal{P}(Y)\rightarrow[0,1]$ such that the following three conditions hold,

$$m_Y(A)\geq 0 \tag{1}$$

$$m_Y(\varnothing)=0 \tag{2}$$

$$\sum_{A\in Y} m_Y(A)=1 \tag{3}$$

As shown in Fig. 1, $m_Y(C_{Y2}) = 5\%$ indicates that 5% portion of one's total belief is assigned to exactly the set $A = C_{Y2} = (t_1, t_2]$. The BPA structure demonstrated in Fig. 1 is formed based on information from one source. If information is from multiple sources, the multiple BPA structures must be aggregated by so-called rules of combination [32].

Similar to a joint probability in probability theory, in evidence theory, if multiple uncertain variables are involved and are independent, then a joint BPA is defined by

$$m_{\mathbf{Y}}(C) = \begin{cases} m_{Y_1}(A) m_{Y_2}(B) & \text{when } C = A \times B \\ 0 & \text{otherwise} \end{cases} \tag{4}$$

where $A \in \mathcal{P}(Y_1)$, $B \in \mathcal{P}(Y_2)$, $\mathbf{Y} = Y_1 \times Y_2$, and $C \in \mathcal{P}(\mathbf{Y})$.

A set *C*, for which $m_{\mathbf{Y}}(C) > 0$, is called a *focal set* (or *focal element*). If the BPA structure of the time to failure of two independent systems 1 and 2 is given in Fig. 2, the joint BPA can be calculated by Eq. (4). For example, $m_{\mathbf{Y}}([0,1],[0,2]) = m_{Y1}([0,1]) m_{Y2}([0,2]) = 0.1(0.25) = 0.025$. The result of the joint BPA is given in Table 1.

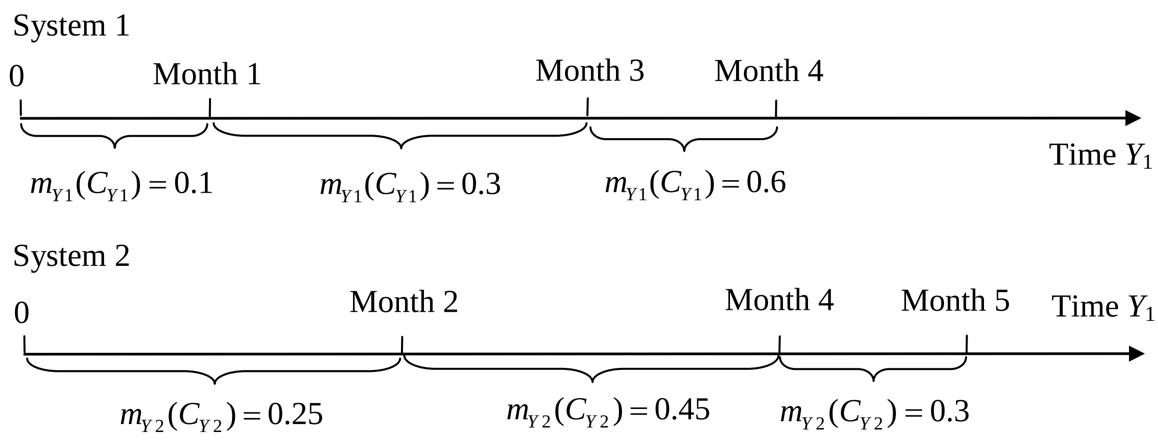

Figure 2. Lives of two systems

Table 1 Joint BPA $m_{\mathbf{Y}}$

Y_2 \ Y_1	$m_{Y1}([0,1]) = 0.1$	$m_{Y1}([1,3]) = 0.3$	$m_{Y1}([3,4]) = 0.6$
$m_{Y2}([0,2]) = 0.25$	0.025	0.075	0.15
$m_{Y2}([2,4]) = 0.45$	0.045	0.135	0.27
$m_{Y2}([4,5]) = 0.3$	0.03	0.09	0.18

Let a response *G* be expressed abstractly by a performance function

$$G = g(\mathbf{Y}) \tag{5}$$

where $\mathbf{Y} = (Y_1, Y_2, \cdots, Y_{n_Y})$ is the vector of parameters with epistemic uncertainty. The uncertainty associated with the model input $\mathbf{Y}$ is propagated through the model $g(\cdot)$ to the model output *G*.

Next we use a reliability problem to conceptually demonstrate how to quantify the effect of epistemic uncertainty. A failure mode *F* is defined as the event that the performance is less than a threshold (a limit state) *c*, i.e. $F = \{\mathbf{Y} | g(\mathbf{Y}) \le c\}$. Due to the interval nature, the likelihood of the failure cannot be quantified by a single probability measure; instead, it is quantified by belief and plausibility measures, which are bounds of the probability.

Let $m_{\mathbf{Y}}$ be the joint BPA over a frame $\mathbf{Y} = Y_1 \times Y_2 \times \cdots \times Y_{n_Y}$. The belief measure *Bel* of the failure event $\mathbf{Y} \in F$ induced by $m_{\mathbf{Y}}$ is defined as follows:

$$Bel(F) = \sum_{A \in F} m_{\mathbf{Y}}(A) \tag{6}$$

$Bel(F)$ is interpreted as the degree of belief that the failure event *F* would occur. The idea is illustrated in Fig. 3. $Bel(F)$ is the sum of the BPAs of the subsets (focal elements) entirely within the failure region $F = \{\mathbf{Y} | g(Y_1, Y_2) \le c\}$. As shown in Fig. 3, subsets $C_{\mathbf{Y}6}$ and $C_{\mathbf{Y}9}$ are completely in the failure region; therefore, $Bel(F) = m_{\mathbf{Y}6} + m_{\mathbf{Y}9} = 0.27 + 0.18 = 0.45$.

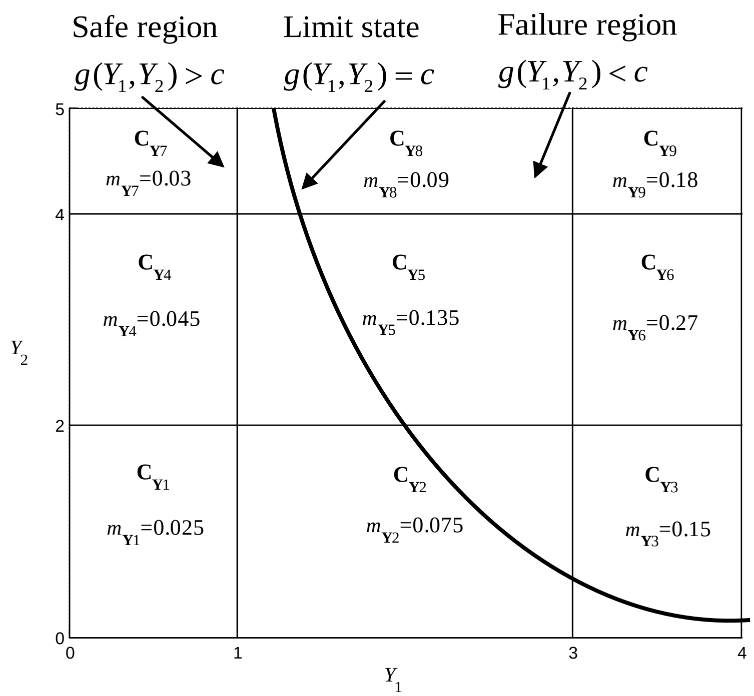

Figure 3. Joint BPA $m_{\mathbf{Y}}$ and the limit state

The plausibility measure *Pl* of the failure mode F induced by $m_{\mathbf{Y}}$ is defined as

$$Pl(F) = \sum_{A \cap F \neq \varnothing} m_{\mathbf{Y}}(A) \tag{7}$$

The degree of plausibility $Pl(F)$ is calculated by adding the BPAs of the subsets that are in the failure region and the BPAs of the subsets that intersect with the failure region. It is obvious that $Pl(F) \ge Bel(F)$. As shown in Fig. 4, the plausibility is

$$
\begin{aligned}
Pl(F) &= \left(m_{\mathbf{Y}2} + m_{\mathbf{Y}5} + m_{\mathbf{Y}8} + m_{\mathbf{Y}3}\right) + \left(m_{\mathbf{Y}6} + m_{\mathbf{Y}9}\right) \\
&= \left(m_{\mathbf{Y}2} + m_{\mathbf{Y}5} + m_{\mathbf{Y}8} + m_{\mathbf{Y}3}\right) + Bel(F) \\
&= \left(0.075 + 0.135 + 0.09 + 0.15\right) + 0.45 = 0.9
\end{aligned}
$$

The true probability of failure p_f is bounded in the interval between $Bel(F)$ and $Pl(F)$, namely,

$$Bel(F) \le p_f \le Pl(F) \tag{8}$$

In the above example, $0.45 \le p_f \le 0.9$.

3. Unified Framework for Uncertainty Analysis

When aleatory and epistemic uncertainties exist, their effects can be quantified with a unified uncertainty analysis framework [33]. Let parameters with aleatory uncertainty $\mathbf{X} = (X_1, X_2, \cdots, X_{n_X})$ be described by probability distributions. For easy demonstration, we assume that the elements of **X** are independent. A performance function is then expressed by

$$G = g(\mathbf{X}, \mathbf{Y}) \tag{9}$$

The theoretical foundation of the unified uncertainty analysis relies on the generality of evidence theory. According to Klir and Wierman [29], a more general theory is capable of capturing uncertainties more faithfully than its less general competitors. However, the more general theory, e.g. evidence theory, requires greater computational demands than the less general theory, e.g. probability theory. The reason is that uncertainty analysis with both aleatory and epistemic uncertainties needs both probabilistic analysis and interval analysis and that both analyses are coupled.

Let the number of the subsets (focal elements) of $\mathbf{Y}$ in the joint space be n and the focal elements of $\mathbf{Y}$ be denoted by $\mathbf{C}_{\mathbf{Y}i}$ $(i=1,2,\cdots,n)$. The probability of failure p_f is defined by

$$p_f = \Pr\{g(\mathbf{X},\mathbf{Y}) < c\} \tag{10}$$

where c is a limit state.

The precise probability p_f is not available because of the intervals in $\mathbf{Y}$, but the minimum and maximum values of p_f , or the belief and plausibility, can be obtained. As shown in [33], the equations of belief and plausibility can be derived from both evidence theory and probability theory as

$$Bel(F) = (p_f)_{\min} = \sum_{i=1}^{n} m_{\mathbf{Y}}(\mathbf{C}_{\mathbf{Y}i}) \Pr\{G_{\max}(\mathbf{X},\mathbf{Y}) < c \mid \mathbf{Y}_i \in \mathbf{C}_{\mathbf{Y}i}\} \tag{11}$$

and

$$Pl(F) = (p_f)_{\max} = \sum_{i=1}^{n} m_{\mathbf{Y}}(\mathbf{C}_{\mathbf{Y}i}) \Pr\{G_{\min}(\mathbf{X},\mathbf{Y}) < c \mid \mathbf{Y}_i \in \mathbf{C}_{\mathbf{Y}i}\} \tag{12}$$

where $G_{\min}(\mathbf{X},\mathbf{Y})$ and $G_{\max}(\mathbf{X},\mathbf{Y})$ are the respective global minimum and maximum values of G in the subset $\mathbf{C}_{\mathbf{Y}i}$.

Eqs. (11) and (12) require that the subsets $\mathbf{C}_{\mathbf{Y}i}$ be mutually exclusive as shown in Fig. 3. However, sets in evidence theory are not necessarily mutually exclusive. If intervals are from multiple information sources or intervals overlap, aggregation needs to be performed. As shown in Ref. 21, through the aggregation, mutually exclusive subsets $\mathbf{C}_{\mathbf{Y}i}$ can be formed.

4. Unified Uncertainty Analysis by the First Order Reliability Method (FORM)

Solving Eqs. 11 and 12 requires interval analysis (IA) to calculate the minimum and maximum performances $G_{\min}$ and $G_{\max}$. It also requires probability analysis (PA) to calculate the probabilities $\Pr\left\{G_{\min}(\mathbf{X},\mathbf{Y})<c \middle| \mathbf{Y}_i \in \mathbf{C}_{\mathbf{Y}i}\right\}$ and $\Pr\left\{G_{\max}(\mathbf{X},\mathbf{Y})<c \middle| \mathbf{Y}_i \in \mathbf{C}_{\mathbf{Y}i}\right\}$. In principle, Monte Carlo simulation (MCS) can be used, but the computation is too expensive. Interval arithmetic could be used for IA to reduce computational efforts, but the method is not accurate and is inapplicable to black-box performance functions. In this section, we introduce our proposed FORM-based unified uncertainty analysis method. The method is efficient than MCS and is applicable to black-box performance functions.

4.1 FORM

FORM is primarily used for probabilistic analysis (PA) when aleatory uncertainty exists with probability distributions. Let the joint probability density function (PDF) of $\mathbf{X}$ be $f_{\mathbf{x}}$. The probability of failure is calculated by the following integral

$$p_f = \Pr\{G = g(\mathbf{X}) < c\} = \int_{g(\mathbf{x})<c} f_{\mathbf{x}}(\mathbf{x})d\mathbf{x} \tag{13}$$

Random variables $\mathbf{X} = \left\{X_1,\ X_2,\ \cdots,\ X_{n_X}\right\}$ (in X-space) are first transformed into a set of random variables $\mathbf{U} = \left\{U_1,\ U_2,\ \cdots,\ U_{n_X}\right\}$ (in U-space) whose elements follow a standard normal distribution. The transformation is given by

$$u_i = \Phi^{-1}\left\{F_{X_i}(x_i)\right\} \tag{14}$$

where F_{X_i} is the CDF of X_i, and Φ^{-1} is the inverse CDF of a standard normal distribution. Then the Most Probable Point (MPP) $\mathbf{u}^*$ is identified with the following model.

$$\min_{\mathbf{u}} \|\mathbf{u}\| \Big| g(\mathbf{u}) = c \tag{15}$$

where $|\cdot|$ stands for the norm (length) of a vector, namely, $\|\mathbf{u}\| = \sqrt{u_1^2 + u_2^2 + \cdots + u_{n_X}^2}$.

p_f is then approximated by

$$p_f = \Phi(-\beta) \tag{16}$$

where Φ is the CDF of a standard distribution.

4.2 The FORM-Based Unified Uncertainty Analysis

Our proposed FORM-based unified uncertainty analysis (FORM-UUA) method evaluates the minimum probability $\Pr\left\{G_{\max}(\mathbf{X},\mathbf{Y}) < c \middle| \mathbf{Y}_i \in \mathbf{C}_{\mathbf{Y}i}\right\}$ for belief in Eq. 11 and the maximum probability $\Pr\left\{G_{\min}(\mathbf{X},\mathbf{Y}) < c \middle| \mathbf{Y}_i \in \mathbf{C}_{\mathbf{Y}i}\right\}$ for plausibility in Eq. 12. The method employs FORM for probabilistic analysis (PA). It also uses nonlinear optimization for interval analysis (IA) to find the minimum and maximum G over the focal element $\mathbf{C}_{\mathbf{Y}i}$. Since both FORM and nonlinear optimization are applicable to black-box performance functions, so is the FORM-UUA method.

Combining the MPP search and interval analysis, the maximum probability $\Pr\left\{G_{\min}(\mathbf{X},\mathbf{Y}) < c \middle| \mathbf{Y}_i \in \mathbf{C}_{\mathbf{Y}i}\right\}$ can be solved by the following model.

$$\min_{\mathbf{u}} \|\mathbf{u}\| \Big| g(\mathbf{u},\mathbf{y}) = c,\ \mathbf{y} \in M = \left\{ \min_{\mathbf{y}}\ g(\mathbf{u},\mathbf{y}) \middle| \mathbf{y} \in C_{Y_i} \right\} \tag{17}$$

For the minimum probability $\Pr\left\{G_{\max}(\mathbf{X},\mathbf{Y}) < c \middle| \mathbf{Y}_i \in \mathbf{C}_{\mathbf{Y}i}\right\}$, M is given by $M = \left\{ \max_{\mathbf{y}}\ g(\mathbf{u},\mathbf{y}) \middle| \mathbf{y} \in C_{Y_i} \right\}$.

A double-loop procedure with fully nested FORM (PA) and optimization (IA) is developed in [33]. The outer loop (PA loop) identifies the MPP in terms of **X** and the inner loop (IA loop) searches the minimum g and maximum G in terms of **Y**. This method is inefficient due to the double-loop procedure. In the FORM-UUA method, IA is embedded in the iterative MPP search process, and the new method is much more efficient.

The FORM-UUA method for the minimum probability $\Pr\left\{G_{\max}(\mathbf{X},\mathbf{Y})<c\,\middle|\,\mathbf{Y}_i\in\mathbf{C}_{\mathbf{Y}i}\right\}$ is outlined in Fig. 4. In each iteration of the MPP search, interval variables **Y** are fixed. After random variables **U** are updated by the MPP search algorithm, optimization is performed to find the maximum performance function with fixed **U**. After the MPP $\mathbf{u}^*$ is located, the maximum probability is computed by

$$\Pr\left\{G_{\max}(\mathbf{X},\mathbf{Y})<c\,\middle|\,\mathbf{Y}_i\in\mathbf{C}_{\mathbf{Y}i}\right\}=\Phi(-\beta) \tag{18}$$

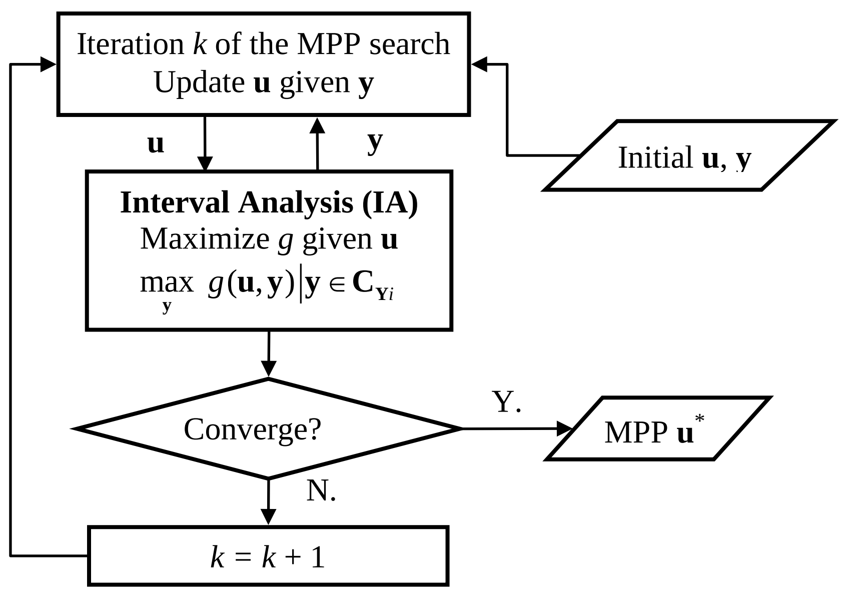

Figure 4. Flowchart of FORM-UUA

An efficient and robust MPP search algorithm is essential to the performance of the FORM-UUA method. The so-call HLRF algorithm [34, 35] is the most popular algorithm owing to its simplicity and efficiency. However, there is no proof that the algorithm will converge for a given problem. It actually diverges for many nonlinear performance functions. In this work, we use the improved version of HLRF algorithm denoted by iHRLF, which is proposed by Zhang and Der Kiureghian [30]. iHRLF is computationally efficient and globally convergent, meaning that it guarantees to converge to a local MPP from any starting point. The detailed algorithm is given in [30]. The adaptation of the algorithm that accommodates interval variables is developed in this work. Next, the algorithm for the minimum probability $\Pr\left\{G_{\max}(\mathbf{X},\mathbf{Y})<c\,\middle|\,\mathbf{Y}_i\in\mathbf{C}_{\mathbf{Y}i}\right\}$ is presented.

In iteration k+1, the MPP is given by

$$\mathbf{u}_{k+1}=\mathbf{u}_k+\alpha\mathbf{d}_k \tag{19}$$

where the search direction $\mathbf{d}_k$ is defined by

$$\mathbf{d}_k=\frac{\nabla g_{\mathbf{y}}(\mathbf{u}_k,\mathbf{y}_k)\mathbf{u}_k^T-g(\mathbf{u}_k,\mathbf{y}_k)}{\left\|\nabla g_{\mathbf{y}}(\mathbf{u}_k,\mathbf{y}_k)\right\|^2}\nabla g_{\mathbf{y}}(\mathbf{u}_k,\mathbf{y}_k)-\mathbf{u}_k \tag{20}$$

where $\nabla g_{\mathbf{y}}(\mathbf{u}_k,\mathbf{y}_k)=\left(\frac{\partial g}{\partial U_1},\frac{\partial g}{\partial U_2},\cdots,\frac{\partial g}{\partial U_n}\right)_{\mathbf{u}_k,\mathbf{y}_k}$.

The step size α is determined by minimizing the merit function defined by

$$m(\mathbf{u},\mathbf{y})=\frac{1}{2}\|\mathbf{u}\|+c\left|g(\mathbf{u},\mathbf{y})\right| \tag{21}$$

in which the constant c should satisfies

$$c > \frac{\|\mathbf{u}\|}{\|\nabla g(\mathbf{u},\mathbf{y})\|} \tag{22}$$

To reduce the computational cost, in practice, the step size is computed by finding a value α that the merit function is sufficiently reduced. The following rule is employed to find α.

$$\alpha = \max_{h\in\mathbb{N}} \left\{ b^h \middle| m(\mathbf{u}_k + b^h\mathbf{d}_k, \mathbf{y}_k) - m(\mathbf{u}_k, \mathbf{y}_k) < 0 \right\},\ b > 0 \tag{23}$$

In the proposed algorithm, $b = 0.5$ and $c = \frac{2\|\mathbf{u}_k\|}{\|\nabla g(\mathbf{u}_k, \mathbf{y}_k)\|} + 10$ are used.

Eq. 23 indicates that $\alpha = h$ is the first integer such that $m(\mathbf{u}_k + b^h\mathbf{d}_k, \mathbf{y}_k)$ is less than $m(\mathbf{u}_k, \mathbf{y}_k)$.

In the above algorithm, interval variables $\mathbf{y}_k$ are assumed fixed, which are obtained from optimization in iteration *k*. Once $\mathbf{u}_{k+1}$ is found, interval analysis is conducted to find $\mathbf{y}_{k+1}$ by the following model.

$$\max_{\mathbf{y}} g(\mathbf{u}_{k+1}, \mathbf{y}) \middle| g(\mathbf{u}_{k+1}, \mathbf{y}) = c,\ \mathbf{y} \in C_{Y_i} \tag{24}$$

In many engineering applications, the extreme values of a performance function occur at the endpoints of interval variables **Y** when the function is monotonic with respect to the interval variables. For example, the maximum design margin is at the maximum strength and minimum loading. In this case, there is no need to perform expensive optimization in Eq. 24. However, it is difficult to know whether a black-box performance function is monotonic. To improve computational efficiency, the following strategy is developed.

In iteration $k+1$, after $\mathbf{u}_{k+1}$ is found, the KKT conditions for the optimization problem at $\mathbf{u}_{k+1}$ in Eq. 24 is checked. If the KKT conditions are satisfied, the interval variables $\mathbf{y}_k$ obtained in iteration k are still the solution to Eq. 24. There is no need to perform optimization again. Therefore, set $\mathbf{y}_{k+1} = \mathbf{y}_k$ and skip optimization, and then proceed to the next iteration.

For the optimization in Eq. 24, the KKT conditions are as follows.

$$H(\mathbf{Y}) = \left\{ j:\ y_j = y_j^L,\ \left.\frac{\partial g(\mathbf{U},\mathbf{Y})}{\partial Y_j}\right|_{\mathbf{u}_{k+1},\mathbf{y}_k} \geq 0 \right\} \bigcup \left\{ j:\ y_j = y_j^U,\ \left.\frac{\partial g(\mathbf{U},\mathbf{Y})}{\partial Y_j}\right|_{\mathbf{u}_{k+1},\mathbf{y}_k} \leq 0 \right\} \quad (25)$$

and

$$\left.\frac{\partial g(\mathbf{U},\mathbf{Y})}{\partial Y_j}\right|_{\mathbf{u}_{k+1},\mathbf{y}_k} = 0,\ j \notin H(\mathbf{Y}) \quad (26)$$

where $j = 1, 2, \cdots, n_Y$, y_j^L is the lower bound of Y_j, and y_j^U is the upper bound of Y_j.

The algorithm is summarized as follows.

(1) Input the starting point $\mathbf{u_0}$ and $\mathbf{y_0}$; initialize the iteration counter k = 0.

(2) Calculate $\mathbf{u}_{k+1}$ by

$$\mathbf{u}_{k+1} = \mathbf{u}_k + \alpha \mathbf{d}_k$$

$$\mathbf{d}_k = \frac{\nabla g_{\mathbf{y}}(\mathbf{u}_k,\mathbf{y}_k)\mathbf{u}_k^T - g(\mathbf{u}_k,\mathbf{y}_k)}{\left\|\nabla g_{\mathbf{y}}(\mathbf{u}_k,\mathbf{y}_k)\right\|^2} \nabla g_{\mathbf{y}}(\mathbf{u}_k,\mathbf{y}_k) - \mathbf{u}_k$$

and

$$\alpha = \max_{h\in\mathbb{N}} \left\{ b^h \,\middle|\, m(\mathbf{u}_k + b^h \mathbf{d}_k, \mathbf{y}_k) - m(\mathbf{u}_k,\mathbf{y}_k) < 0 \right\},\ b > 0$$

(3) If $k > 1$, check KKT conditions in Eqs. 25 and 26. If satisfied, $\mathbf{y}_{k+1} = \mathbf{y}_k$ and go to (5); otherwise, go to (4).

(4) Find $\mathbf{y}_{k+1}$ by solving $\max_{\mathbf{y}} g(\mathbf{u}_{k+1}, \mathbf{y}) \big| g(\mathbf{u}_{k+1}, \mathbf{y}) = c,\ \mathbf{y} \in C_{Y_i}$.

(5) Check convergence. If $\left| g(\mathbf{u}_{k+1}, \mathbf{y}_{k+1}) - c \right| \le \varepsilon_1$ and $\left\| \mathbf{u}_{k+1} - \mathbf{u}_k \right\| \le \varepsilon_2$ (ε_1 and ε_2 are small positive numbers $\ll 1.0$), then $\beta = \left\| \mathbf{u}_{k+1} \right\|$ and go to (6); otherwise, $k = k + 1$, go to (2).

(6) $\Pr\left\{ G_{\max}(\mathbf{X}, \mathbf{Y}) < c \,\middle|\, \mathbf{Y}_i \in \mathbf{C}_{\mathbf{Y}i} \right\} = \Phi(-\beta)$ when $G(\mathbf{u}_{k+1}, \mathbf{y}_{k+1}) \ge c$; $\Pr\left\{ G_{\max}(\mathbf{X}, \mathbf{Y}) < c \,\middle|\, \mathbf{Y}_i \in \mathbf{C}_{\mathbf{Y}i} \right\} = \Phi(\beta)$ when $G(\mathbf{u}_{k+1}, \mathbf{y}_{k+1}) < c$.

The flowchart of the above procedure is depicted in Fig. 5.

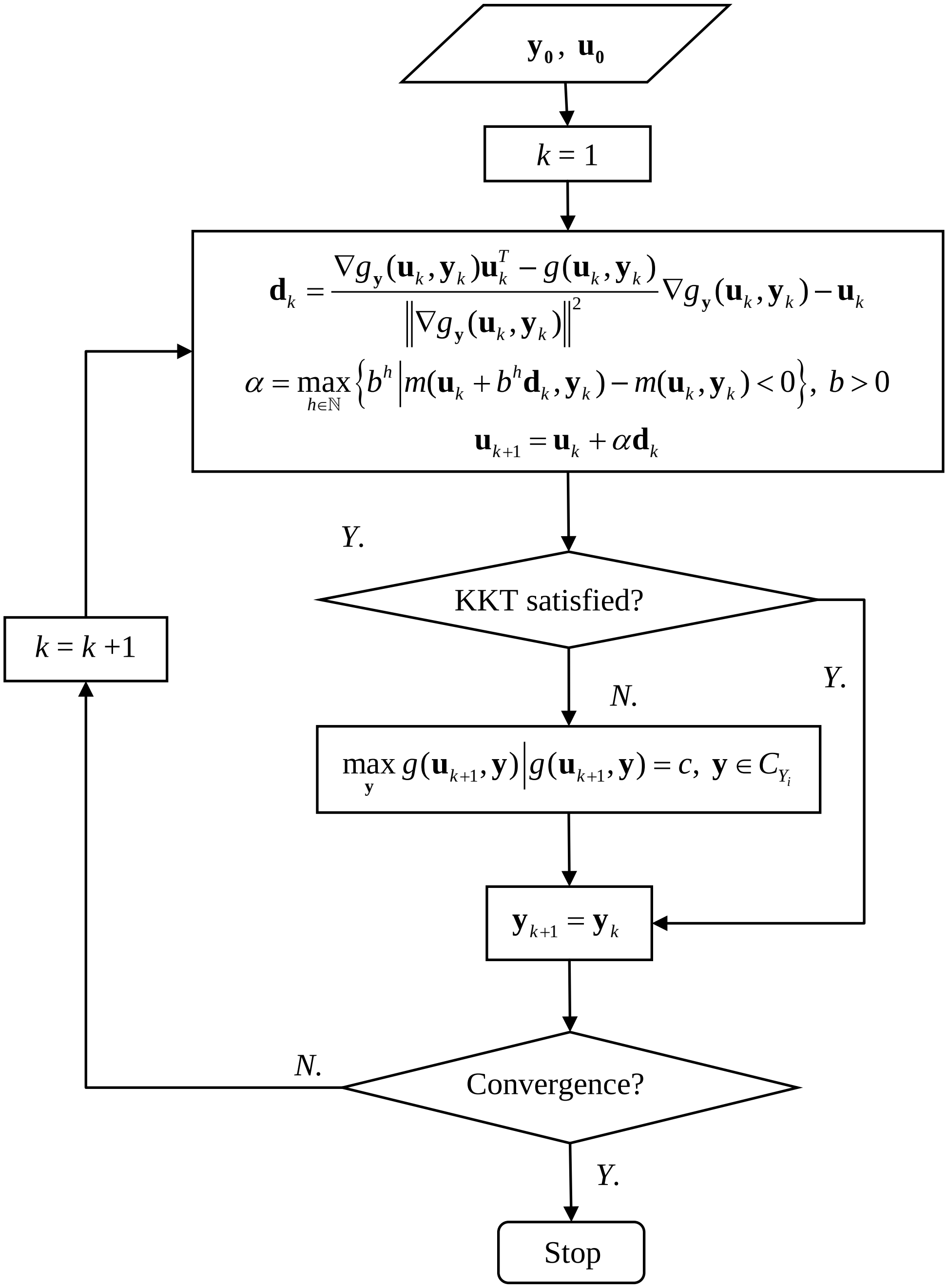

Figure. 5 Flowchart of the FORM-UUA Method

For the maximum probability $\Pr\left\{G_{\min}(\mathbf{X},\mathbf{Y})<c\,\middle|\,\mathbf{Y}_i\in\mathbf{C}_{\mathbf{Y}i}\right\}$, one just needs to change the optimization model for interval analysis to $\min_{\mathbf{y}} g(\mathbf{u}_{k+1},\mathbf{y})\,\middle|\, g(\mathbf{u}_{k+1},\mathbf{y})=c,\ \mathbf{y}\in C_{Y_i}$.

The proposed method converges in a few iterations. If the number of iterations is *m*, the whole procedure solves the minimization and maximization problem *m* times for interval analysis if the solution includes an interior point over an interval. The efficiency of solving the minimization (or maximization) problem depends on the number of interval variables **Y** and features of the performance function. The computational cost of the MPP search is directly proportional to the number of random variables **X** if the finite difference method is used to evaluate derivatives. In general, the computational demand of the entire process is dependent upon the numbers of intervals and random variables. Since the above process must be performed for each of the focus elements of **Y**, the overall efficiency is also determined by the number of the focal elements.

5. Numerical Examples

The proposed FORM-UUA method is coded in MATLAB. The sequential Quadratic Programming (SQP) optimizer is used to solve interval analysis. Two engineering problems are used here for demonstration. Even though the performance functions in both examples are in analytical forms, they are coded as executable programs and are therefore implicit to the calling function. The derivatives of the performance functions with respect to random variables and interval variables are computed by the forward finite element approach. A black-box situation is therefore simulated.

5.1 Crank-slide mechanism

A crank-slider mechanism (Fig. 6) is used in a construction machine. The length of the crank *a*, the length of the coupler *b*, the external force *P*, the Young's modulus of the material of the coupler *E*, and the yield strength of the coupler *S* are random variables. The distributions of the random variables are given in Table 2.

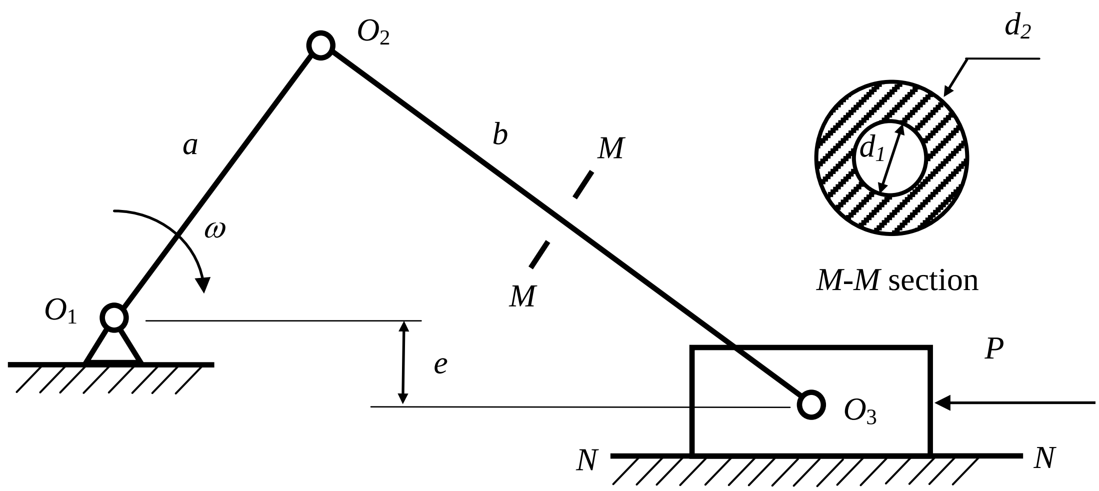

Figure 6. A Crank-Slider Mechanism

Table 2 Random Variables X

Variable	Symbol used in Fig. 6	Mean	Standard deviation	Distribution
X_1	*a*	100 mm	0.01 mm	Normal
X_2	*b*	400 mm	0.01 mm	Normal
X_3	*P*	280 kN	28 kN	Normal
X_4	*E*	200 GPa	10 GPa	Normal
X_5	*S*	290 MPa	29 MPa	Normal

Because of the harsh environment in construction sites, a precise distribution of the coefficient of friction μ between the ground and the slider is unknown; only its intervals and BPA are available from the solicitation from experts. Different installation positions of the slider are required in various construction sites. The intervals and BPA of the offset e are assigned based on limited historical data. Their BPAs are provided in Table 3.

Table 3 Uncertain Variables with Epistemic Uncertainty

Variable	Symbol used in Fig. 6	Intervals	BPA
Y_1	e	[100, 120], [120, 140] , [140, 150]	0.2, 0.4, 0.4
Y_2	μ	[0.15, 0.18], [0.18, 0.23], [0.23, 0.25]	0.3, 0.3, 0.4

The two performance functions are defined by the difference between the material strength and the maximum stress, and the difference between the critical load and the axial load, respectively. They are given by

$$G_1 = g_1(\mathbf{X}, \mathbf{Y}) = S - \frac{4P(b-a)}{\pi\left(\sqrt{(b-a)^2 - e^2} - \mu e\right)\left(d_2^2 - d_1^2\right)}$$

and

$$G_2 = g_2(\mathbf{X}, \mathbf{Y}) = \frac{\pi^3 E\left(d_2^4 - d_1^4\right)}{64b^2} - \frac{P(b-a)}{\sqrt{(b-a)^2 - e^2} - \mu e}$$

The failure events are defined by $F_1 = \{\mathbf{X}, \mathbf{Y} | g_1(\mathbf{X}, \mathbf{Y}) < 0\}$ and $F_2 = \{\mathbf{X}, \mathbf{Y} | g_2(\mathbf{X}, \mathbf{Y}) < 0\}$. The belief and plausibility measures of failure are computed by the proposed FORM-UUA approach, and the results are given in Table 4. The true probability of failure of the first response is bounded with the belief and plausibility measures, i.e. $4.36\times10^{-5} \le p_{f1} \le 1.38\times10^{-4}$. Because both belief and plausibility measures are almost zero for the second response, the probability of failure for the second performance function $p_{f2} \approx 0$. Both performance functions are monotonic with respect to the interval variables e and μ, and the extreme function values occur at the endpoints of the two interval variables. Therefore, optimization for interval analysis is performed only in the first iteration of the MPP search and is skipped thereafter. The reason is that the FORM-UUA detects that the KKT conditions are satisfied. The total numbers of function calls for the two performance functions are 522 and 576, respectively. To compare the accuracy, Monte Carlo simulation (MCS) is also used to solve the problem. MCS is applied to the four combinations of the endpoints of e and μ. 10^6 samples are used for each combination. The results indicate the good accuracy of the proposed method with the MCS solution as a reference.

Table 4 Belief and Plausibility Measures

Failure	Belief *Bel*		Plausibility *Pl*		N_1	N_2
	FORM-UUA	MCS	FORM-UUA	MCS		
F_1	4.36×10^{-5}	4.44×10^{-5}	1.38×10^{-4}	1.44×10^{-4}	522	4×10^6
F_2	≈ 0	0.0	≈ 0	0.0	576	4×10^6

N_1 – number of function evaluations by the FORM-UUA method
N_2 – number of function evaluations by MCS

The cumulative belief function (CBF) and cumulative plausibility function (CPF) are also calculated by changing the constant c in both $F_1 = \{\mathbf{X}, \mathbf{Y} | g_1(\mathbf{X}, \mathbf{Y}) < c\}$ and $F_2 = \{\mathbf{X}, \mathbf{Y} | g_2(\mathbf{X}, \mathbf{Y}) < c\}$. The results are depicted in Figs. 7 and 8. The gap between the CBF and CPF of G_1 is much larger than that of G_2. This indicates that the effect of epistemic uncertainty on G_1 is greater than that on G_2. The difference between the CBF and CPF of G_2 is small. Therefore, the effect of epistemic uncertainty on G_2 is not significant.

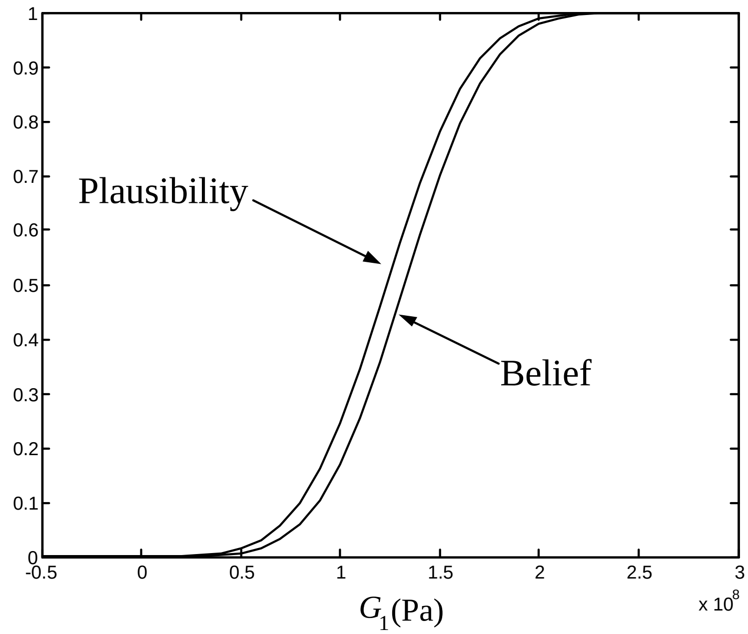

Figure 7. CBF of G_1

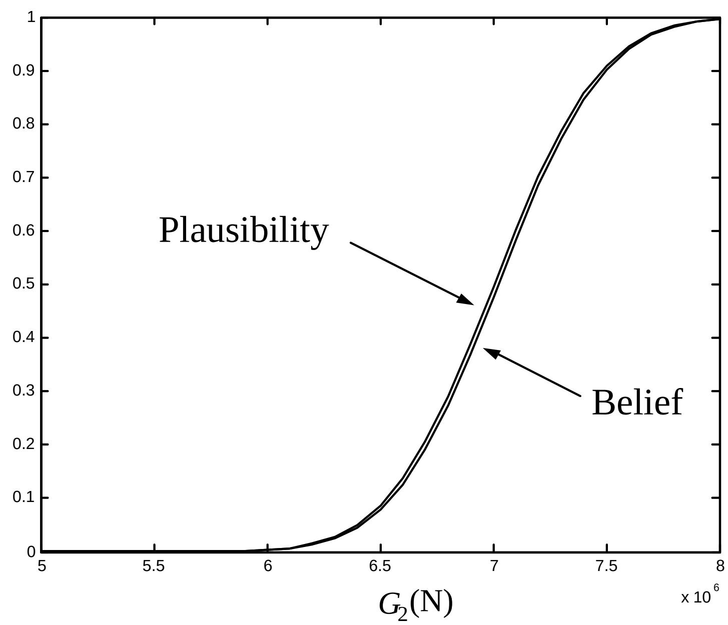

Figure 8. CPF of G_2

5.2 Cantilever tube

The cantilever tube shown in Fig. 9 is subjected to external forces F_1, F_1, and P, and torsion T. The performance function is defined as the difference between the yield strength S_y and the maximum stress σ_y, namely,

$$G = g(\mathbf{X,Y}) = S_y - \sigma_{\max}$$

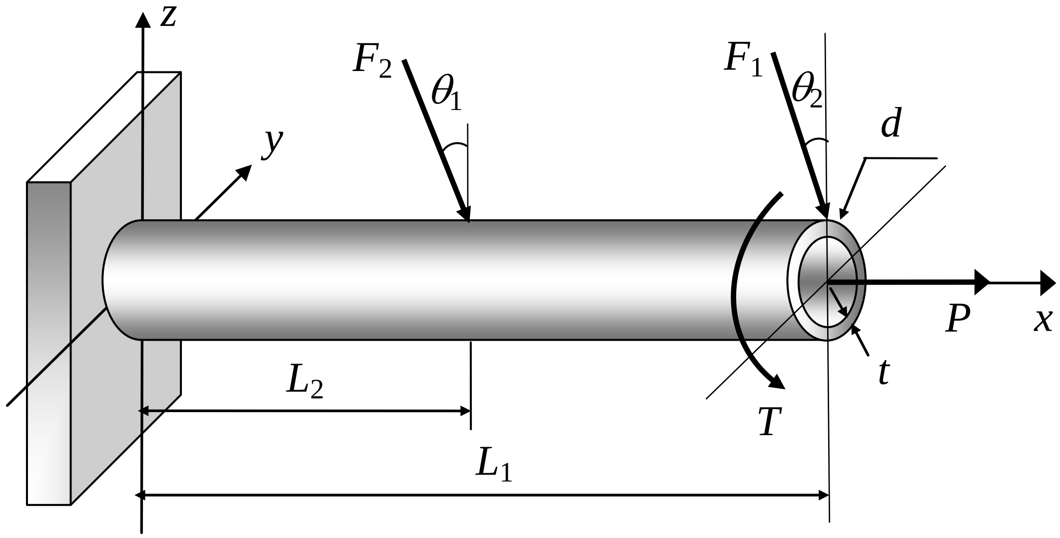

Figure 9. Cantilever Tube

$\sigma_{\max}$ is the maximum von Mises stress on the top surface of the tube at the origin, which is given by

$$\sigma_{\max} = \sqrt{\sigma_x^2 + 3\tau_{zx}^2}$$

The normal stress σ_x is calculated by

$$\sigma_x = \frac{P + F_1 \sin(\theta_1) + F_2 \sin(\theta_2)}{A} + \frac{Mc}{I}$$

where the first term is the normal stress due to the axial forces, and the second term is the normal stress due to the bending moment *M*, which is given by

$$M = F_1 L_1 \cos(\theta_1) + F_2 L_2 \cos(\theta_2) ,$$

and

$$A = \frac{\pi}{4}\left[d^2 - (d-2t)^2\right],\ c = d/2,\ I = \frac{\pi}{64}\left[d^4 - (d-2t)^4\right].$$

The torsional stress τ_{zx} at the same point is calculated by

$$\tau_{zx} = \frac{Td}{2J}$$

where

$$J = 2I$$

The random and interval variables are given in Tables 5 and 6, respectively.

Table 5 Uncertain Variables with Aleatory Uncertainty

Variables	Symbols in Fig. 10	Parameter 1	Parameter 2	Distribution
X_1	t	5 mm (mean)	0.1 mm (std*)	Normal
X_2	d	42 mm (mean)	0.5 mm (std)	Normal
X_3	L_1	119.75 mm (lb**)	120.25 mm (ub***)	Uniform
X_4	L_2	59.75 mm (lb)	60.25 mm (ub)	Uniform
X_5	F_1	3.0 kN (mean)	0.3 kN (std)	Normal
X_6	F_2	3.0 kN (mean)	0.3 kN (std)	Normal
X_7	P	12.0 kN (mean)	1.2 kN (std)	Gumbel
X_8	T	90.0 N·m (mean)	9.0 N·m (std)	Normal
X_9	S_y	220.0 MPa (mean)	22.0 MPa (std)	Normal

*: std – standard deviation
**: lb – lower bound of a uniform distribution
***: ub – upper bound of a uniform distribution

Table 6 Uncertain Variables with Epistemic Uncertainty

Variables	Symbols in Fig. X	Intervals	BPA
Y_1	θ_1	[0°, 10°]	1.0
Y_2	θ_2	[5°, 15°]	1.0

The bounds of the probability of failure of the cantilever tube are calculated by the proposed method and are shown in Table 7. The result is compared with that of MCS. As demonstrated in Figs. 10 and 11, the minimum performance occurs at the interior points of

θ_1 and θ_2. To capture the minimum value of the performance function in MCS, the intervals of θ_1 and θ_2 are divided into 50 subintervals. 50×50 combinations of the two interval variables are simulated with 10^6 samples for each combination. The total number of MCS function calls is therefore equal to $50\times50\times10^6 = 2.5\times10^9$. With the MCS solution as a reference, the proposed method is accurate and efficient.

Table 7 Belief and Plausibility Measures

Failure	Belief *Bel*		Plausibility *Pl*		N_1	N_2
	FORM-UUA	MCS	FORM-UUA	MCS		
F	0.000143	0.000145	0.000163	0.000168	147	2.5×10^9

N_1 – number of function evaluations by the FORM-UUA method
N_2 – number of function evaluations by MCS

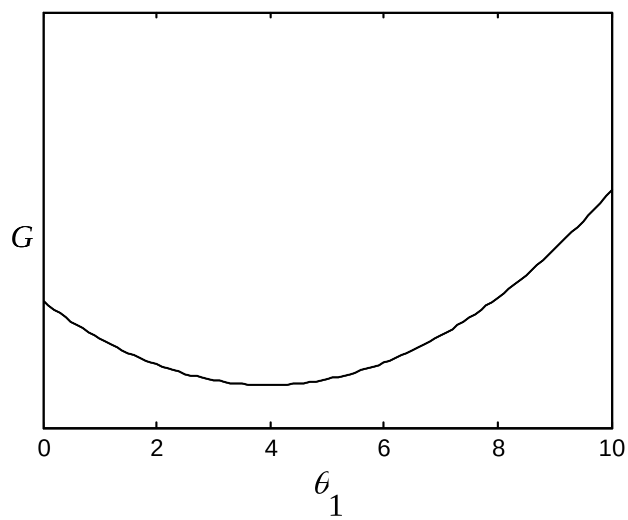

Figure 10. G-θ_1 at the means of random variables and the average of θ_2

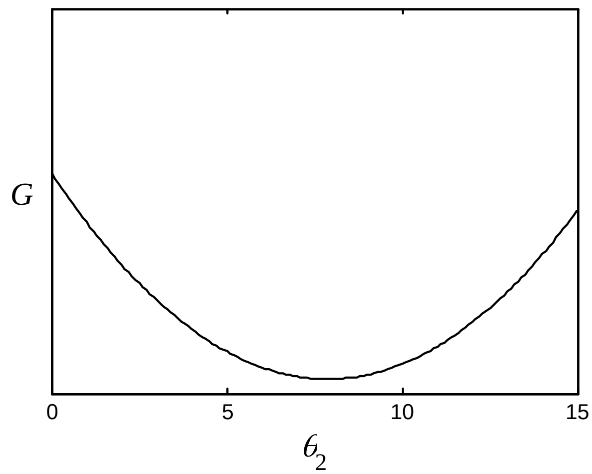

Figure 11. G-θ_2 at the means of random variables and the average of θ_1

To show the effect of the epistemic uncertainty in θ_1 and θ_2 for a full range of the performance, we also plot the CBF and CPF in Fig. 12. Since the gap between the two curves is small, the effect of the epistemic uncertainty is not significant.

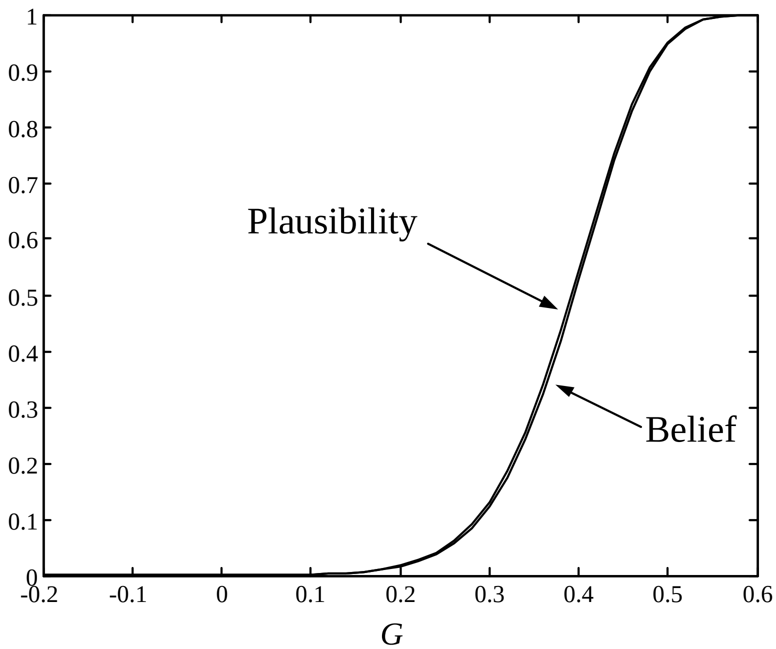

Figure 12. CBF and CPF of *G*

6. Conclusions and Future Work

The feasibility of performing unified uncertainty analysis using existing reliability method FORM is demonstrated in this paper. Given probability distributions of aleatory parameters **X** and joint basic probability assignments of epistemic parameters **Y**, the belief measure and plausibility measure of a response variable $G = g(\mathbf{X}, \mathbf{Y})$ can be easily calculated. It is shown that the calculation of belief measure or plausibility measure can be converted to the calculation of the minimum or maximum probability of failure (or the CDF of *G*) at each focal element of **Y**. As a result, the unified uncertainty analysis needs a number of probabilistic analyses and interval analyses.

As shown in the two examples, both belief and plausibility measures provide more insight into the uncertainty impact on design performance than a single probability measure. The values of both measures indicate the effect of aleatory uncertainty on a response while the gap between them reflects the effect of epistemic uncertainty on the response. Considering both types of uncertainty helps us make more informed decisions.

Let us examine the following two cases for reliability issue. In case 1, the belief and plausibility measures about a failure event are large, and so is the effect of aleatory uncertainty; the gap between belief and plausibility measures small, so is the effect of epistemic uncertainty. In this case, we may focus on using our limited resources to deal with safety issues for the most critical components in a system. In case 2, the effect of epistemic uncertainty is large because of a large gap between belief and plausibility measures. In this case, simply using the worst case probability (plausibility) may result in a very conservative solution; it is also difficult to make decisions due to the large gap. In this case, the available resources should be used to reduce epistemic uncertainty by performing experiments or collecting more information. The sensitivity information from the unified uncertainty analysis will guide one to collect more information for the most critical epistemic variables and their combinations before making decisions.

The proposed FORM-UUA method enables us to propagate both aleatory and epistemic uncertainties in the model input to the model output for a black-box model. It is practical to use the algorithm to calculate the belief or plausibility measure for a single limit state. If it is used to generate the entire CBF and CPF curves, the MPP for each of the realizations of the response must be searched. As the result, the computation will be intensive.

It should be pointed out that the iHLRF algorithm can identify only a single local MPP. If there are multiple MPPs or the MPP search converges to a local MPP, the FORM-UUA method may produce a large error. If the nonlinear optimization for interval analysis does not converge to a global optimal solution, the error may also be large. In this case, a global optimizer may be considered. The starting points of the MPP search and interval analysis have large influence upon the overall performance of the FORM-UUA method. In this paper, we use the origin of the transformed normal space as the starting point for the MPP search. We use the optimal point of interval analysis from previous MPP search iteration as the starting point for interval analysis in the next iteration of MPP search.

This work has demonstrated the feasibility of integrating probability and evidence theories for handling two types of uncertainty computationally. However, the following several prominent open issues must be resolved before the unified uncertainty analysis can be confidently used in engineering practices.

(1) The unified uncertainty analysis with both types of uncertainty is much more computationally expensive than probabilistic analysis. The proposed method is only a starting point. More efficient and accurate approximation methods should be developed.

(2) As seen in the two example problems, Monte Carlo simulation is extremely costly for the unified uncertainty analysis. Practical simulation techniques need to be investigated. One of the challenging issues is the extreme values of the response over the intervals of epistemic uncertainty may be missed even though large sample size is used. The current sampling methods for epistemic uncertainty should be further developed to overcome the drawback.

(3) Sensitivity information should be a byproduct of the unified uncertainty analysis. Sensitivity analysis identifies the contributions of individual uncertain input variables to the output. Especially, the sensitivity of the gap between the lower and upper probability bounds of a response needs to be calculated because it provides the most useful information for reducing epistemic uncertainty.

(4) How to formulate the joint BPA as the input to the unified uncertainty analysis is not addressed in this paper. When the information of epistemic uncertainty comes from multiple sources, the following question should be answered? How should multiple estimates of uncertain quantities be aggregated before uncertainty analysis calculation?

(5) Results from the unified uncertainty analysis helps engineers understand how the mixture of both aleatory and epistemic uncertainties impacts design performance. This knowledge will ultimately be used at the design stage for mitigating such impact. Effectively integrating the unified uncertainty analysis with design schemes in both modeling and computational implementation should be the focus of the future research.

Acknowledgement

This work is partially supported by the U.S. National Science Foundation grant CMMI – 040081 and the University of Missouri – Rolla Intelligent Systems Center. The support is gratefully acknowledged. The author would also like to thank the four anonymous reviewers for their valuable comments and suggestions.

Reference

[1] Chong, K.P, Saigal, S., Thynell, S., and Morgan, H.S., 2002, "Research Needs," in Modeling and Simulation-Based Life Cycle Engineering, Spon Press, New York.

[2] Zang, T.A., Hemsch, M.J., Hilburger, M.W., Kenny, S.P., Luckring, J.M., Maghami P., Padula, S.L., and Stroud, W.J., 2002, "Needs and Opportunities for Uncertainty-Based Multidisciplinary Design Methods for Aerospace Vehicles," NASA/TM-2002-211462.

[3] Cafeo, J.A., Donndelinger, J.A., Lust, R.V., and Mourelatos, Z.P., 2005, "The Need for Nondeterministic Approaches in Automotive Design: A Business Perspective," in Engineering Design Reliability Handbook, edited by Nilolaidis, E., Chiocel, D.M., and Singhal, S., CRC Press, Washington D.C.

[4] Nikolaidis, E., 2005, "Types of Uncertainty in Design Decision Making," in: Engineering Design Reliability Handbook, edited by Nikolaidis, E., Ghiocel D.M., and Singhal, S., CRC Press, New York.

[5] Mourelatos, Z. and Zhou, J., 2004, "Reliability Estimation and Design with Insufficient Data Based on Possibility Theory," 10th AIAA/ISSMO Multidisciplinary Analysis and Optimization Conference, Albany, New York.

[6] Oberkampf, W. L., and Helton, J. C., 2002, "Investigation of Evidence Theory for Engineering Applications," 4th Non-Deterministic Approaches Forum, Denver, Colorado.

[7] Dewooght, J., 1998, “Model Uncertainty and Model Inaccuracy,” Reliability Engineering and System Safety, 59(2), 171–185.

[8] Apley, D.W., Liu, J., and Chen, W., 2006, “Understanding the Effects of Model Uncertainty in Robust Design With Computer Experiments,” ASME Journal of Manufacturing Science and Engineering, 128(4), 657-1022.

[9] Mahadevan, S. and Rebba, R., 2006, “Inclusion of Model Errors in Reliability-Based Optimization,” ASME Journal of Manufacturing Science and Engineering, 128(4), 936-944.

[10] Chen, W., Allen, J.K., Tsui, K-L, and Mistree, F., “A Procedure for Robust Design,” ASME Journal of Mechanical Design, 118 (4), 478-485, 1996.

[11] Hernandez, G., Simpson, T., Allen, J., Bascaran, E., Avila L., and Salinas, F., 2001, “Robust Design of Families of Products with Production Modeling and Evaluation,” ASME Journal of Mechanical Design, 123(2), 183-190.

[12] Kanukolanu, D., Lewis, K., and Winer, E., 2004, “Robust Design of Coupled Sub-Systems Using Visualization,” 41st AIAA Aerospace Sciences Meeting and Exhibit, January 2004, Reno, NV.

[13] Frey, D.D. and Li, X., 2004, “Validating Robust Parameter Design Methods,” ASME 2004 Design Engineering Technical Conferences and Computer and Information in Engineering Conference, Salt Lake City, Utah, USA, September 28 – October 2.

[14] Messac, A. and Sundararaj, G.J., 2000, “A robust design approach using Physical Programming,” 38th Aerospace Sciences Meeting and Exhibit, Reno, NV.

[15] Du, X. and Chen, W., 2004, “Sequential Optimization and Reliability Assessment for Probabilistic Design,” ASME Journal of Mechanical Design, 126(2), 225-233.

[16] Allen, M. and Maute, K., 2004, “Reliability-Based Design Optimization of Aeroelastic Structures,” Structural and Multidisciplinary Optimization, 27(4), 228-242.

[17] Tu, J., Choi, K.K., and Young H.P., 1999, “A New Study on Reliability-Based Design Optimization,” ASME Journal of Mechanical Engineering, 121(4), 557-564.

[18] Mavris, D.N., Bandte, O., and DeLaurentis, D.A., 1999, "Robust Design Simulation: A Probabilistic Approach to Multidisciplinary Design," AIAA Journal of Aircraft, 36(1), 298-307.

[19] Gu, X., Renaud, J.E., Batill, S.M., Brach, R.M., and Budhiraja, A., 2000, "Worst Case Propagated Uncertainty of Multidisciplinary Systems in Robust Optimization", Structural Optimization, 20(3), pp. 190-213.

[20] Yu, X. and Du, X., 2006, "Reliability-Based Multidisciplinary Optimization for Aircraft Wing Design," Structure and infrastructure Engineering: Maintenance, Management, Life-Cycle Design and Performance, 2(3/4), 277-289.

[21] Soundappan, P., Nikolaidis, E., Haftka, R.T., Grandhi, R., and Canfield, R., 2004, "Comparison of Evidence Theory and Bayesian Theory for Uncertainty Modeling," Reliability Engineering and System Safety, 85(1-3), 295-311.

[22] Nikolaidis, E., Chen, C., Cudney, H., Haftka, R.T., and Rosca, R., 2003, "Comparison of Probability and Possibility for Design Against Catastrophic Failure Under Uncertainty," ASME Journal of Mechanical Design, 126(3), 386-394.

[23] Ling, J.M., Aughenbaugh, J.M., and Paredis, C.J.J., 2006, "Managing the Collection of Information Under Uncertainty Using Information Economics," ASME Journal of Mechanical Design, 128(4), 980-990.

[24] Du, L., Choi, K.K., Youn, B.D., and Gorsich, D., 2006, "Possibility-Based Design Optimization Method for Design Problems with Both Statistical and Fuzzy Input Data," ASME Journal of Mechanical Design, 128(4), 928-935.

[25] Mourelatos, Z.P. and Zhou J., 2006, "A Design Optimization Method Using Evidence Theory," ASME Journal of Mechanical Design, 128(4), 901-908.

[26] Bae1, H.-R., Grandhi, R.V., and Canfield, R.A., 2006, "Sensitivity Analysis of Structural Response Uncertainty Propagation Using Evidence Theory," Structural and Multidisciplinary Optimization, 31(4), 270-279.

[27] Agarwal, H., Renaud, J.E., Preston, E.L., and Padmanabhan, D., 2004, "Uncertainty Quantification Using Evidence Theory in Multidisciplinary Design Optimization," Reliability Engineering and System Safety, 85(1-3), 281-294.

[28] Bae H.-R., Grandhi, R.V., and Canfield R.A., 2004, "Epistemic uncertainty quantification techniques including evidence theory for large-scale structures," Computers and Structures, 82(13-14): 1101–1112.

[29] Klir, G.J. and Wierman, M.J., 1999, Uncertainty-Based Information – Elements of Generalized Information Theory, Physics-Verlag, Heidelberg, New York.

[30] Zhang Y. and der Kiureghian A, 1995, "Two Improved Algorithms for Reliability Analysis," Reliability and Optimization of Structural Systems, Proceedings of the Sixth IFIP WG7.5 Working Conference on Reliability and Optimization of Structural Systems, Assisi, Italy, September 7-9, 1994.

[31] Du, X., Sudjianto, A., and Huang, B., 2005, "Reliability-Based Design under the Mixture of Random and Interval Variables," ASME Journal of Mechanical Design, 127(6), 1068-1076.

[32] Klir, G.J., 2005, Uncertainty and Information – Foundations of Generalized Information Theory, John Wiley & Sons, Inc., Hoboken, New Jersey.

[33] Du, DETC Du, X., 2006, "Uncertainty Analysis with Probability And Evidence Theories," The 2006 ASME International Design Engineering Technical Conferences & Computers and Information In Engineering Conference, September 10-13, Philadephia, U.S.A.

[34] Hasofer, A.M. and Lind, N.C., 1974, "Exact and Invariant Second-Moment Code Format," *Journal of the Engineering Mechanics Division, ASCE*, 100(EM1), pp. 111-121.

[35] Rackwits, R. and Fiessler, B., 1978, "Structural Reliability under Combined Random Load Sequences," Computers and Structures, 9(5): 484-494.